PROCEEDINGS OF SPIE

SPIEDigitalLibrary.org/conference-proceedings-of-spie

Plasmonic nanogap structures studied via cathodoluminescence imaging

Stephen J. Bauman
Qigeng Yan
Mourad Benamara
Joseph B. Herzog

SPIE.

Plasmonic nanogap structures studied via cathodoluminescence imaging

Stephen J. Bauman[a], Qigeng Yan[b], Mourad Benamara[c], Joseph B. Herzog[*,a,b]

[a]Microelectronics-Photonics Program, University of Arkansas, Fayetteville, AR, 72701, USA;
[b]Department of Physics, University. of Arkansas, Fayetteville, AR, 72701, USA;
[c]Institute for Nanoscience and Engineering, University of Arkansas, Fayetteville AR 72701, USA

ABSTRACT

Cathodoluminescence makes use of the beam raster capabilities of a scanning electron microscope to excite electrons in a sample and collects the luminescent light to produce images or obtain spectra that can reveal useful information about the sample. This technique has been shown to be particularly interesting for studying the plasmonic oscillations of metallic nanostructures. A recently developed fabrication technique has allowed for the creation of sub-10 nm gaps between metallic nanostructures for use as plasmonically active samples that can be tailored for various potential applications. The high degree of control over the geometries capable of being fabricated via this nanomasking technique allow for unique types of structures that are otherwise difficult to fabricate. In this work, the plasmonic response of metallic structures separated by sub-10 nm gaps is studied via CL imaging. Hyperspectral images can demonstrate the effectiveness with which various geometries produce specific wavelength resonances. The results can be helpful in determining which structures are optimal for specific applications based on these resonances. Also, the images can help to guide future fabrication, as the plasmon modes become better understood.

Keywords: Plasmonics, surface plasmons, metallic nanostructure, cathodoluminescence

1. INTRODUCTION

Fabrication and characterization of plasmonic nanostructures are important for the development of devices such as plasmonically enhanced sensors, photodetectors, and photovoltaics.[1–7] Improved fabrication capabilities enable the production of novel geometries, use of hybrid materials, and other advancements not possible decades ago at the advent of theoretical plasmonics work.[8–11] Two benefits of modern fabrication capabilities are the creation of extremely small (sub-100 nm) nanostructures and sub-10 nm gaps between these structures, especially important for plasmonic enhancement applications.[12–16] The nanomasking fabrication technique is a recently developed method for creating metallic nanostructures on a substrate surface with geometrical control and the ability to produce sub-10 nm gaps between individual structures.[17] The technique can be utilized via standard lithography processes, making it suitable for applications requiring mass production. Nanostructure geometries that have not before been easy to fabricate with lithographic processes have been demonstrated by this technique and studies are underway to test their applicability as substrates for SERS sensors and photodetectors.[18–20] The optimization of nanomasking-patterned plasmonic structures for such applications will be aided by experimental spectroscopic data of fabricated samples. One powerful method of spectroscopic analysis for studying plasmonic resonances is cathodoluminescence imaging/spectroscopy.

Cathodoluminescence (CL) uses an accelerated electron beam, typically as part of a scanning electron microscope (SEM), impinging on a sample surface to excite electrons, causing emission of light upon their relaxation. CL can also be used to study plasmonic resonances of metallic structures by using the SEM beam to excite plasmons and image the structures.[21–25] Figure 1 depicts the CL process and the setup for obtaining images and spectra. The electron beam is scanned across the sample and at each location of the beam, light is given off depending on the excitability of the structure at that beam position. The light given off by this resonance is collected via a parabolic mirror inserted into the vacuum chamber along with the sample and the electron optics. The light can be sent directly to a photomultiplier tube (PMT) for panchromatic imaging, diffracted via a grating and sent to a charge-couple device (CCD) camera to obtain the full spectra, or diffracted and passed through a monochromator slit to the PMT to obtain a "single" wavelength signal. If the diffracted light is collected by the CCD in what is known as parallel mode, hyperspectral images of the sample can

* Email: jbherzog@uark.edu

Plasmonics: Design, Materials, Fabrication, Characterization, and Applications XV,
edited by Din Ping Tsai, Takuo Tanaka, Proc. of SPIE Vol. 10346, 1034607

be obtained. This data cube is powerful in analyzing plasmonic modes and the locations at which they are most readily excited. CL has been used in the study of plasmon resonances in metallic nanostructures of various sizes under different conditions, as well as for materials characterization studies.

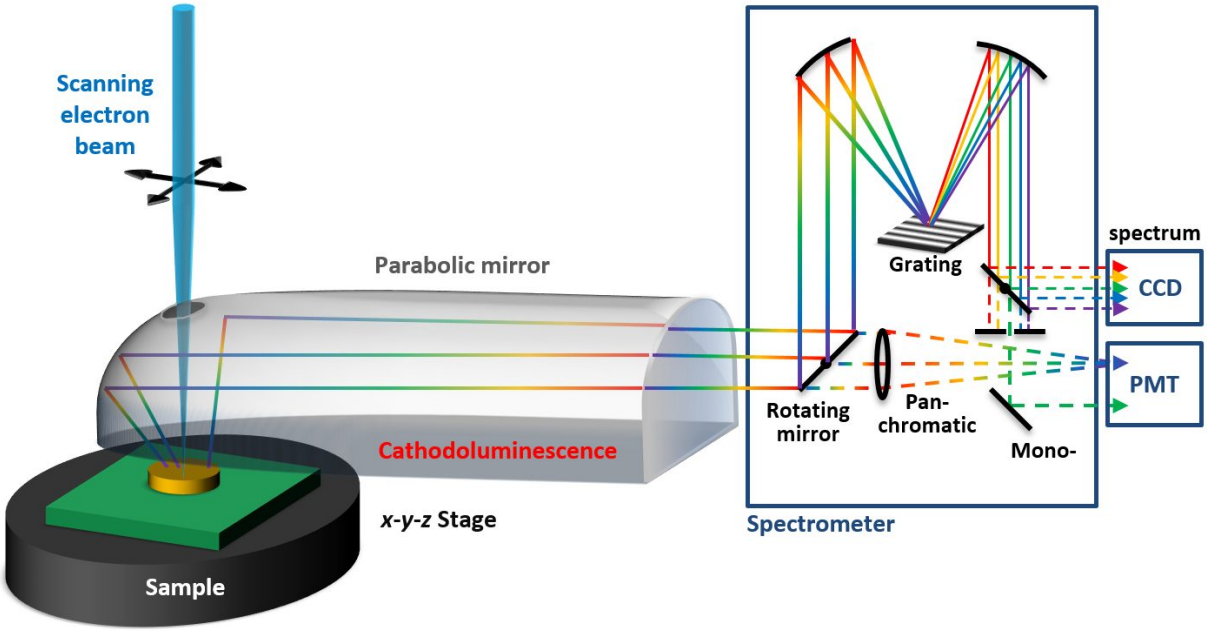

Figure 1. Schematic of the cathodoluminescence (CL) setup. The scanning electron beam is shown impinging on a metal nanostructure on the sample surface, causing CL photons to be emitted. The parabolic mirror is shown directing the photons to the spectrometer where they are either sent directly to the PMT (panchromatic mode) or to the diffraction grating to spread the wavelengths spatially. If the grating is used, the diffracted light is sent either to the CCD to obtain the full spectrum and/or hyperspectral images (parallel mode) or passed through a slit to the PMT (monochromatic mode).

The PMT and CCD can be used to create an excitability map, generated in much the same way as the image obtained via the secondary electron detector in a SEM. The sketches in Figure 2 depict the concept of excitability allowing the creation of these maps. The electron beam strikes a specific point on the sample, the location of a single pixel in the CL image. With the beam focused on a given location, electrons are excited and subsequent photons emitted at nearby sample locations. It is important to note that the total signal is comprised of photons emitted not only from the exact beam position, but from locations all around the sample surface near the beam position. As one example, Figure 2(a) depicts the beam striking the center of one of the nanostructures, causing some CL emission from the sample. Figure 2(b) shows the beam impinging on the edge of the center nanostructure and the resulting increase in the CL emission strength. The parabolic mirror redirects the same hemispherical area of emitted light in both cases, resulting in a stronger measured signal at the CCD/PMT for (b) than for (a). Thus, pixel by pixel, a map of the sample's excitability can be constructed, with areas emitting more CL photons represented by brighter pixels.

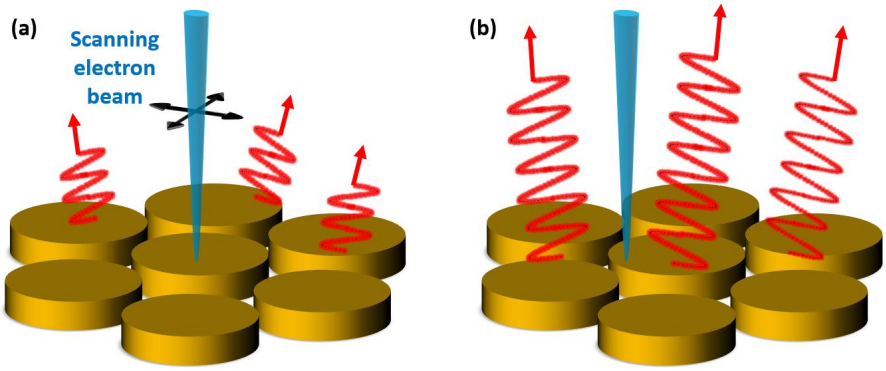

Figure 2. Illustration demonstrating the generation of excitability maps. (a) The electron beam impinges on the middle of the center nanostructure, causing the emission of CL photons from the entire sample region. (b) The beam impinges on the edge of the center nanostructure, causing a stronger CL emission response, again from the entire local sample area.

2. CATHODOLUMINESCENCE RESULTS

Cathodoluminescence experiments have been performed at the University of Arkansas using a Gatan Mono CL4 system connected to a FEI Nova Nanolab 600 DualBeam (FIB/SEM). The system is capable of panchromatic imaging, taking point by point spectra and thereby creating hyperspectral images, and creating monochromatic images, as demonstrated by the image in Figure 1. Preliminary example images of the CL system's panchromatic capability are shown in Figure 3. Metallic nanostructures were fabricated via electron beam lithography on Si/SiO_2 substrates. Here, the oxide layer was 100 nm thick, and a 1 nm Ti layer was used to adhere the 80 nm Au layer to the substrate. A SEM image of a single nanostructure is shown in Figure 3(a), and the corresponding CL image is shown in (b). A CL map of a circular heptamer structure like the sketches in Figure 2 is shown in Figure 3(c). The panchromatic excitability of square structures in a checkered pattern are shown in Figure 3(d). In (b) – (d), the excitability maps have been colorized for clarity, with bright yellow/white representing more photon counts and blue representing less. The exact count values are not shown here, as the figure is merely illustrating the locations of greatest excitation.

The CL maps in Figure 3 provide a preliminary look at the plasmonic resonances of the structures shown. The excitability is greatest when the electron beam is focused at the edges of the Au structures. Interesting to note in Figure 3(c) and (d) is that the excitability is greatest for the metallic structure edges nearest to the neighboring nanostructures. This is a strong indication that plasmonic resonances play a significant role in the emission of CL for these metallic structures. This type of analysis will prove useful in testing the optimization of various fabricated structures in future work.

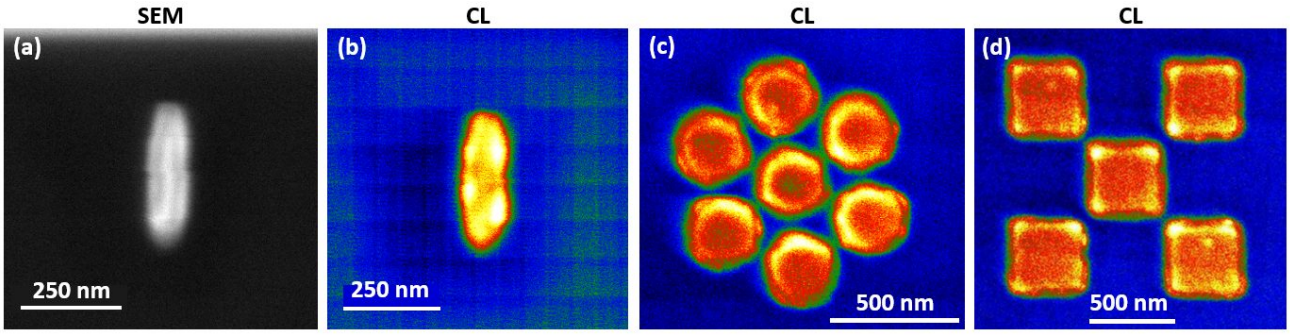

Figure 3. (a) SEM image and (b) – (d) colorized, preliminary, panchromatic cathodoluminescence (CL) images of various nanostructures.

Samples were fabricated on two different substrates in these preliminary tests, one containing a 100 nm thermally grown SiO_2 layer and the other a native oxide layer of approximately 1 nm. Panchromatic images and spectra were obtained for similar nanostructures on each sample and compared as shown in Figure 4. The 100 nm oxide sample is shown in Figure

4(a) and the native oxide results in (b). The panchromatic CL images are shown for each case in (i) and the spectra, obtained over slightly different ranges, have been aligned by wavelength in (ii). The 100 nm oxide demonstrated more contrast than the native oxide sample, as seen by the difference in the CL maps in (a) and (b). Also notable are the differences in the spectra for each case. It is interesting to note these substrate effects, as recent computational optimization work by Bauman et al. has demonstrated similar dependence on the substrate oxide layer for optical responses.[20] This is thought to be related to a thin-film interference effect between the substrate and the plasmonic structures. In Figure 4(a-ii), the total number of counts is much greater for the peaks exhibited by the sample at 450 and 640 nm, and the signal to noise ratio is lower than that in (b-ii). Also, the peaks are narrower for the 100 nm oxide sample. The peaks are red-shifted by approximately 60 nm for the native oxide sample in (b-ii), exhibiting much lower signal to noise and broadened peak-widths. For the native oxide sample in (b-ii), the 640 nm peak in (a-ii) has also flattened significantly to appear as barely more than a shoulder on the shorter wavelength peak. More data and further analysis are required to fully interpret the significance of these results and their implications toward optimization of the nanostructures and substrates for various applications.

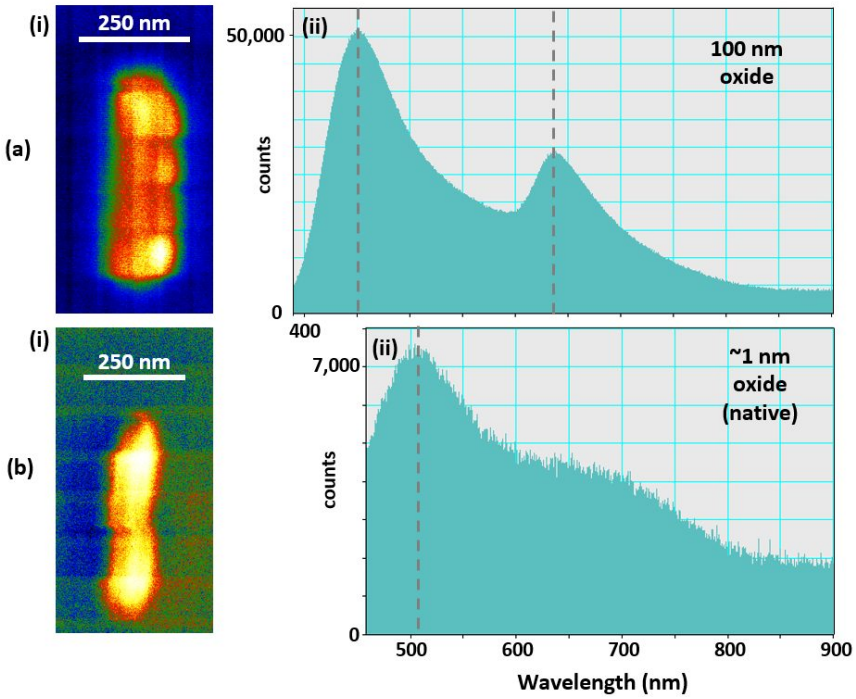

Figure 4. Preliminary comparison of two 80 nm thick Au nanostructures with comparable dimensions on Si substrates containing (a) a 100 nm SiO2 layer and (b) a native oxide layer (~1 nm). Panchromatic CL (i) images and (ii) spectra with the peak locations emphasized by the dashed gray lines.

3. CONCLUSION

The capability of utilizing cathodoluminescence imaging and spectroscopy for the study of plasmonic nanostructures at the University of Arkansas Electron Optics Facility has been demonstrated. Panchromatic images and spectra have been obtained for various Au nanostructures, and a preliminary comparison of the effects of different substrate oxide thicknesses has been performed. The effects of a thicker oxide on the CL results include increased image contrast, spectral peak shifts, and increased signal to noise ratio in the spectrum. Future work to study the CL response of plasmonic structures will help to further characterize these effects and will aid in the optimization stage of developing plasmonic devices such as sensors and photodetectors. This work will help pave the way for future CL experiments, both internal and collaborative, as well as aiding in the study of various materials and devices via this powerful technique.

ACKNOWLEDGEMENTS

Funding has been provided by the National Science Foundation Grant award numbers 1460754 and 359306. Funding for this research has been provided by the Department of Physics, the Fulbright College of Arts and Sciences, and the Vice Provost for Research and Economic Development at the University of Arkansas. Stephen J. Bauman has been supported by the Doctoral Academy Fellowship through the University of Arkansas Graduate School and the SPIE Optics + Photonics Education Scholarship.

REFERENCES

1. G. B. Jung et al., "Nanoplasmonic Au nanodot arrays as an SERS substrate for biomedical applications," *Appl. Surf. Sci.* ***282***, 161–164 (2013) [doi:10.1016/j.apsusc.2013.05.093].
2. A. G. Brolo, "Plasmonics for future biosensors," *Nat. Photonics* ***6****(11)*, 709–713 (2012) [doi:10.1038/nphoton.2012.266].
3. T. Chung et al., "Plasmonic Nanostructures for Nano-Scale Bio-Sensing," *Sensors* ***11****(11)*, 10907–10929 (2011) [doi:10.3390/s111110907].
4. A. Karar et al., "High-responsivity plasmonics-based GaAs metal-semiconductor-metal photodetectors," *Appl. Phys. Lett.* ***99****(13)*, 133112 (2011) [doi:10.1063/1.3625937].
5. A. I. Nusir et al., "Near-infrared metal-semiconductor-metal photodetector based on semi-insulating GaAs and interdigital electrodes," *Photonics Res.* ***3****(1)*, 1 (2015) [doi:10.1364/PRJ.3.000001].
6. V. E. Ferry, J. N. Munday, and H. A. Atwater, "Design Considerations for Plasmonic Photovoltaics," *Adv. Mater.* ***22****(43)*, 4794–4808 (2010) [doi:10.1002/adma.201000488].
7. S. Ahn, D. Rourke, and W. Park, "Plasmonic nanostructures for organic photovoltaic devices," *J. Opt.* ***18****(3)*, 33001 (2016) [doi:10.1088/2040-8978/18/3/033001].
8. M. Altissimo, "E-beam lithography for micro-/nanofabrication," *Biomicrofluidics* ***4****(2)*, 26503 (2010) [doi:10.1063/1.3437589].
9. H. Duan et al., "Direct and Reliable Patterning of Plasmonic Nanostructures with Sub-10-nm Gaps," *ACS Nano* ***5****(9)*, 7593–7600 (2011) [doi:10.1021/nn2025868].
10. A. Biswas et al., "Advances in top–down and bottom–up surface nanofabrication: Techniques, applications & future prospects," *Adv. Colloid Interface Sci.* ***170****(1–2)*, 2–27 (2012) [doi:10.1016/j.cis.2011.11.001].
11. M. Ito et al., "Simultaneous fabrication of nanogaps using field-emission-induced electromigration," *in 2014 International Conference on Manipulation, Manufacturing and Measurement on the Nanoscale (3M-NANO)*, pp. 312–315 (2014) [doi:10.1109/3M-NANO.2014.7057331].
12. J. Chen et al., "One-step fabrication of sub-10-nm plasmonic nanogaps for reliable SERS sensing of microorganisms," *Biosens. Bioelectron.* ***44***, 191–197 (2013) [doi:10.1016/j.bios.2013.01.038].
13. A. P. Edwards and A. M. Adawi, "Plasmonic nanogaps for broadband and large spontaneous emission rate enhancement," *J. Appl. Phys.* ***115****(5)*, 53101 (2014) [doi:10.1063/1.4864018].
14. X. Chen et al., "Nanogap-Enhanced Infrared Spectroscopy with Template-Stripped Wafer-Scale Arrays of Buried Plasmonic Cavities," *Nano Lett.* ***15****(1)*, 107–113 (2015) [doi:10.1021/nl503126s].
15. H. Cai et al., "Wafer scale fabrication of highly dense and uniform array of sub-5 nm nanogaps for surface enhanced Raman scatting substrates," *Opt. Express* ***24****(18)*, 20808 (2016) [doi:10.1364/OE.24.020808].
16. Y. Li, M. L. Simeral, and D. Natelson, "Surface-Enhanced Infrared Absorption of Self-Aligned Nanogap Structures," *J. Phys. Chem. C* ***120****(39)*, 22558–22564 (2016) [doi:10.1021/acs.jpcc.6b07851].
17. S. J. Bauman et al., "Fabrication of Sub-Lithography-Limited Structures via Nanomasking Technique for Plasmonic Enhancement Applications," *IEEE Trans. Nanotechnol.* ***14****(5)*, 790–793 (2015) [doi:10.1109/TNANO.2015.2457235].
18. A. A. Darweesh, S. J. Bauman, and J. B. Herzog, "Improved optical enhancement using double-width plasmonic gratings with nanogaps," *Photonics Res.* ***4****(5)*, 173 (2016) [doi:10.1364/PRJ.4.000173].
19. Z. T. Brawley et al., "Modeling and optimization of Au-GaAs plasmonic nanoslit array structures for enhanced near-infrared photodetector applications," *J. Nanophotonics* ***11****(1)*, 016017–016017 (2017) [doi:10.1117/1.JNP.11.016017].

20. S. J. Bauman et al., "Substrate Oxide Layer Thickness Optimization for a Dual-Width Plasmonic Grating for Surface-Enhanced Raman Spectroscopy (SERS) Biosensor Applications," *Sensors **17**(7)*, 1530 (2017) [doi:10.3390/s17071530].
21. E. J. R. Vesseur et al., "Direct Observation of Plasmonic Modes in Au Nanowires Using High-Resolution Cathodoluminescence Spectroscopy," *Nano Lett. 7(9)*, 2843–2846 (2007) [doi:10.1021/nl071480w].
22. T. Suzuki and N. Yamamoto, "Cathodoluminescent spectroscopic imaging of surface plasmon polaritons in a 1-dimensional plasmonic crystal," *Opt. Express **17**(26)*, 23664–23671 (2009) [doi:10.1364/OE.17.023664].
23. K. Takeuchi and N. Yamamoto, "Visualization of surface plasmon polariton waves in two-dimensional plasmonic crystal by cathodoluminescence," *Opt. Express **19**(13)*, 12365–12374 (2011) [doi:10.1364/OE.19.012365].
24. T. Coenen, E. J. R. Vesseur, and A. Polman, "Angle-resolved cathodoluminescence spectroscopy," *Appl. Phys. Lett. **99**(14)*, 143103 (2011) [doi:10.1063/1.3644985].
25. J. B. Herzog et al., "Dark Plasmons in Hot Spot Generation and Polarization in Interelectrode Nanoscale Junctions," *Nano Lett. **13**(3)*, 1359–1364 (2013) [doi:10.1021/nl400363d].